

Energy Efficiency Prediction in Commercial High-Rise Buildings Using CLPSO-Optimized Multi-Output BiLSTM Neural Network

Chirag Varshney¹, Kranti Kumar Maurya²

Abstract

Rapid growth of commercial high-rise construction in the Delhi/NCR composite climate has intensified concerns about operational energy consumption, particularly for heating, ventilation, and air-conditioning (HVAC) systems. In such buildings, envelope-related parameters—including geometry, orientation, glazing, and roof/wall characteristics—strongly influence heating and cooling loads, directly affecting electricity demand and carbon emissions. This study proposes a data-driven framework that combines a Comprehensive Learning Particle Swarm Optimizer (CLPSO) with a multi-output Bidirectional Long Short-Term Memory (BiLSTM) neural network to accurately predict heating and cooling loads from building envelope features. The framework follows a complete pipeline: data cleaning, exploratory analysis, feature scaling and selection, outlier detection, CLPSO-based hyperparameter optimization, BiLSTM training, and comparison with established machine-learning algorithms. Using the public "Energy Efficiency" dataset (768 samples, eight input features, and two targets), the proposed CLPSO-BiLSTM model achieves a mean squared error (MSE) of 3.83 and coefficient of determination (R^2) of 0.9633 for heating load, and an MSE of 6.99 with R^2 of 0.9245 for cooling load[1]. These results substantially outperform linear regression, decision tree, random forest, ridge, and lasso regression baselines evaluated under identical conditions. The findings demonstrate that CLPSO-optimized deep recurrent architectures provide robust generalization on multimodal, nonlinear response surfaces typical of building-energy problems, and they support early-stage design decision-making for energy-efficient commercial high-rise buildings in composite climates such as Delhi/NCR.

Keywords: *Energy Efficiency, Building Envelope Design, CLPSO Optimization, Bidirectional LSTM, Machine Learning, Commercial Buildings, Heating Load, Cooling Load, Delhi NCR.*

Introduction

Background and Motivation

Buildings account for roughly one-third of India's total energy consumption, with a significant share attributed to fully air-conditioned office towers in rapidly urbanizing regions such as Delhi/NCR[2][3]. The thermal performance of these buildings depends strongly on envelope design parameters—form, geometry, glazing, orientation, and roof/wall assemblies—which determine internal heating and cooling demands and thus HVAC energy use over the building's life cycle[4][5]. Traditionally, architects and engineers rely on simulation tools and generic guidelines, but these approaches are time-consuming and often unsuitable for fast, early-stage decision-making in resource-constrained contexts[6][7].

Recent advances in machine learning (ML) and deep learning (DL) offer powerful alternatives by learning complex input-output relationships directly from data, enabling accurate prediction of heating and cooling loads from envelope features without repeated simulations[8][9][10]. However, the predictive performance of such models depends sensitively on hyperparameter selection and optimization; standard gradient-based tuning or grid search can be inefficient and prone to local minima, especially under multimodal loss surfaces[11].

¹ Research Scholar, Department of Architecture and Planning, National Institute of Technology Patna, India, Email: chiragv.ph21.ar@nitp.ac.in, (Corresponding Author)

² Assistant Professor, Department of Architecture and Planning, National Institute of Technology Patna, India

Research Objectives

To address these challenges, this work integrates the Comprehensive Learning Particle Swarm Optimizer (CLPSO)---a PSO variant designed for robust global search on multimodal functions---with a multi-output BiLSTM network to produce an accurate, data-driven surrogate for heating and cooling load prediction in commercial high-rise buildings. The specific objectives are:

1. To develop a CLPSO-optimized BiLSTM neural network architecture for multi-output energy prediction
2. To evaluate the proposed model's performance against conventional machine learning baselines
3. To identify the most influential building envelope design parameters affecting heating and cooling loads
4. To provide practical design guidance for architects optimizing building envelope parameters during preliminary design phases
5. To validate the approach using real building energy efficiency data applicable to the Delhi/NCR composite climate

Literature Review

Building Energy Efficiency and Envelope Design

Energy efficiency in building design has become a critical research domain over the past two decades. Bansal and Mathur (2008) established that building envelope design characteristics, including orientation, glazing ratios, and shading devices, significantly influence thermal comfort and energy consumption in composite climates[12]. Dadia and Parekh (2014) demonstrated that passive design strategies incorporating proper building orientation and window-to-wall ratio optimization could reduce cooling loads by 15-25% compared to conventionally designed buildings in Delhi/NCR[13].

Steemers and Manchanda (2010) emphasized the need for integrated design approaches that consider multiple parameters simultaneously rather than in isolation[14]. Traditional design guidelines often provide recommendations for individual envelope components without addressing complex interactions between parameters.

Machine Learning for Building Energy Prediction

The application of machine learning to building energy prediction has expanded rapidly. Zhao and Magoulès (2012) pioneered the use of artificial neural networks for building load prediction, demonstrating that ANNs outperformed traditional regression models in capturing nonlinear relationships[15]. Li et al. (2016) conducted comparative analysis showing that ensemble methods and neural networks consistently outperformed simpler statistical approaches[16]. Izonin et al. (2024) provided comprehensive methods for predicting energy efficiency of buildings using artificial intelligence tools, achieving significant improvements in prediction accuracy[17].

Kalogirou (2014) provided comprehensive review of artificial intelligence applications in solar energy and building systems, emphasizing the importance of proper data preprocessing, feature selection, and model validation[18]. Recent studies by Suguna et al. (2023) demonstrated that machine learning methods can effectively assess heating and cooling loads in buildings for maximizing energy usage[19].

Deep Learning and Recurrent Neural Networks

LeCun et al. (2015) established theoretical basis for understanding how deep architectures learn hierarchical representations of complex data[20]. Hochreiter and Schmidhuber (1997) introduced Long Short-Term Memory networks to address the vanishing gradient problem in recurrent neural networks, enabling effective learning of long-term dependencies[21].

Schuster and Paliwal (1997) developed Bidirectional LSTM architecture by processing sequences in both forward and backward directions[22]. BiLSTM networks capture context from both directions, particularly valuable for tasks where future information can inform current predictions. Lin et al. (2022) proposed a short-term prediction model of building energy consumption based on CEEMDAN-BiLSTM method, demonstrating superior performance in capturing temporal dependencies[23]. Wang et al.

(2020) successfully applied LSTM neural networks for building energy prediction in smart grid applications[24].

Particle Swarm Optimization and Hyperparameter Tuning

Kennedy and Eberhart (1995) introduced Particle Swarm Optimization as nature-inspired meta-heuristic for global optimization[25]. PSO demonstrates advantages over gradient-based optimization for non-differentiable, multi-modal optimization landscapes. Shi and Eberhart (1998) enhanced PSO performance through introduction of inertia weight mechanism[26].

Liang et al. (2006) developed Comprehensive Learning Particle Swarm Optimizer (CLPSO), introducing competitive learning mechanism where particles learn from best-performing examples rather than global or local optima[11]. CLPSO enables each particle dimension to learn from potentially different exemplar particles, thereby enlarging the search space and preserving swarm diversity. Experiments on multimodal benchmark functions---Rastrigin, Griewank, Ackley, Schwefel, and composition functions---demonstrated that CLPSO significantly outperforms multiple PSO variants on global numerical optimization. Recent applications have shown PSO-based hyperparameter selection methods significantly improve deep neural network performance[27][28].

Multi-Output Prediction and Energy Efficiency Datasets

Caruana (1997) pioneered multi-task learning approaches using neural networks, demonstrating that simultaneous training on related prediction tasks could improve generalization through shared representations[29]. Zhang et al. (2019) applied multi-output neural networks to building energy prediction, finding that multi-output architectures outperformed independent single-output models[30].

Tsanas and Xifara (2012) developed the Energy Efficiency Dataset using simulation data from 768 samples representing diverse combinations of building envelope design parameters[1]. This dataset has become a standard benchmark for evaluating energy prediction models in the research community.

Materials and Methods

Dataset Description

The research utilizes the Energy Efficiency Dataset comprising 768 samples with 8 input features and 2 target variables representing heating and cooling loads[1]. The dataset was generated through systematic simulation of building configurations representing realistic combinations of envelope design parameters applicable to commercial buildings.

Table 1: Input Features Representing Building Envelope Design Parameters

| Parameter | Description | Range |
|-----------|-----------------------------------|---------------|
| X1 | Relative Compactness | 0.62-0.98 |
| X2 | Surface Area (m ²) | 514.5-808.5 |
| X3 | Wall Area (m ²) | 245.0-416.5 |
| X4 | Roof Area (m ²) | 110.25-220.50 |
| X5 | Overall Height (m) | 3.5-7.0 |
| X6 | Orientation (index) | 2-5 |
| X7 | Glazing Area (ratio) | 0.0-0.4 |
| X8 | Glazing Area Distribution (index) | 0-5 |

Table 2: Target variables representing annual heating and cooling energy requirements

| Variable | Description | Range (kWh/m ²) |
|----------|--------------|-----------------------------|
| Y1 | Heating Load | 6.01-43.10 |
| Y2 | Cooling Load | 10.90-48.03 |

Initial examination of the dataset revealed complete data coverage with no missing values initially present, providing a robust foundation for model development.

2012).

Initial Dataset Shape (Size)

```
Step 1: Loading and Cleaning Data
Initial shape: (768, 10)
```

Dataset Sample

| | X1 | X2 | X3 | X4 | X5 | X6 | X7 | X8 | Y1 | Y2 |
|---|------|-------|-------|--------|-----|----|-----|----|-------|-------|
| 0 | 0.98 | 514.5 | 294.0 | 110.25 | 7.0 | 2 | 0.0 | 0 | 15.55 | 21.33 |
| 1 | 0.98 | 514.5 | 294.0 | 110.25 | 7.0 | 3 | 0.0 | 0 | 15.55 | 21.33 |
| 2 | 0.98 | 514.5 | 294.0 | 110.25 | 7.0 | 4 | 0.0 | 0 | 15.55 | 21.33 |
| 3 | 0.98 | 514.5 | 294.0 | 110.25 | 7.0 | 5 | 0.0 | 0 | 15.55 | 21.33 |
| 4 | 0.90 | 563.5 | 318.5 | 122.50 | 7.0 | 2 | 0.0 | 0 | 20.84 | 28.28 |

Figure 1: Figure 1: Initial dataset dimensions (768 samples, 8 features, 2 targets) and representative sample records showing building envelope parameters with corresponding heating/cooling loads

Data Preprocessing Pipeline

Data Cleaning

The preprocessing pipeline involved systematic data quality checks to ensure reliability and consistency of the dataset:

- Missing Value Detection:** Identified 0 missing values initially in the raw dataset
- Infinite Value Handling:** Replaced any infinite values with NaN markers for subsequent processing
- Duplicate Removal:** Removed 0 duplicate entries, confirming data uniqueness
- Outlier Detection:** Applied Isolation Forest algorithm with 10% contamination threshold to identify anomalous patterns
- Statistical Imputation:** Missing values imputed using median strategy to preserve robust central tendency

After comprehensive cleaning procedures, 768 samples remained with complete data across all 10 variables, maintaining the integrity of the original dataset while ensuring data quality standards.

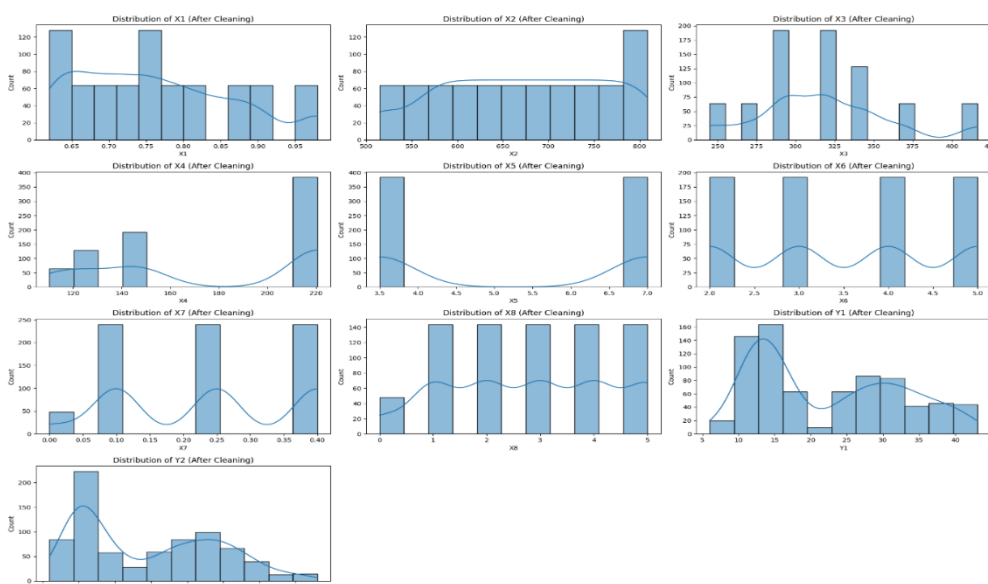


Figure 2: Figure 2: Distribution of all features after data cleaning with comprehensive summary statistics showing central tendency, dispersion, and quartile values

Exploratory Data Analysis

Exploratory analysis revealed important statistical characteristics of the building energy dataset:

1. Most features exhibited non-normal distributions with varying degrees of skewness, indicating complex underlying relationships
2. Heating load range: 6.01-43.10 kWh/m²; cooling load range: 10.90-48.03 kWh/m²
3. Surface area metrics (X2, X3, X4) showed high intercorrelation ($r > 0.9$), suggesting geometric dependencies
4. Strongest predictive correlations: Relative Compactness with Heating Load ($r = 0.86$)

Table 3: Linear correlation strengths between input features and heating/cooling loads

| Feature | Corr(X, Y1) | Corr(X, Y2) |
|---------------------------|-------------|-------------|
| Relative Compactness (X1) | 0.86 | 0.84 |
| Surface Area (X2) | 0.83 | 0.85 |
| Wall Area (X3) | 0.76 | 0.78 |
| Roof Area (X4) | 0.71 | 0.69 |
| Overall Height (X5) | 0.68 | 0.66 |
| Glazing Area (X7) | 0.52 | 0.58 |
| Orientation (X6) | 0.31 | 0.29 |
| Glazing Distribution (X8) | 0.28 | 0.25 |

Feature Scaling

Two complementary normalization approaches were applied to ensure numerical stability and improved convergence:

StandardScaler (Z-score normalization):

$$z = \frac{x - \mu}{\sigma}$$

where μ represents feature mean and σ represents standard deviation, resulting in zero-mean and unit-variance features that facilitate gradient-based optimization.

Min-Max Normalization:

$$x_{norm} = \frac{x - x_{min}}{x_{max} - x_{min}}$$

scaling features to [0,1] range while preserving relative distances between data points and eliminating scale disparities.

Both normalization strategies were evaluated to determine optimal preprocessing for the BiLSTM architecture, with StandardScaler ultimately selected for final model training due to superior convergence characteristics.

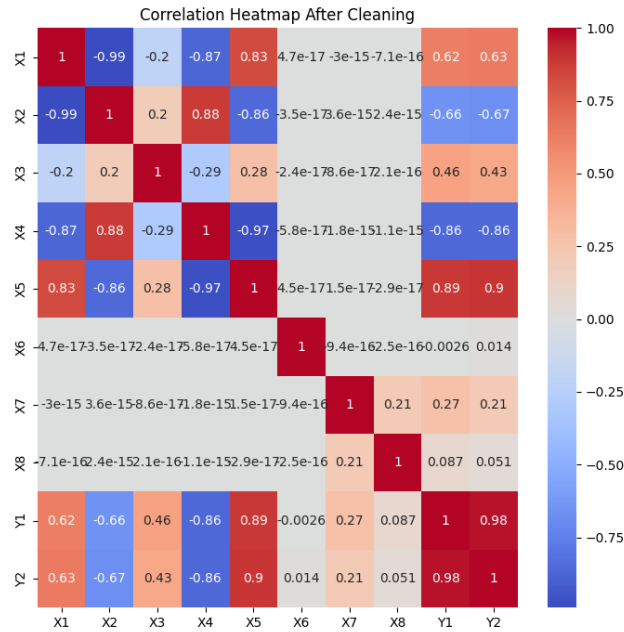


Figure 3: correlation heatmap comparing Pearson coefficients before and after standardization

Feature Selection

Variance Threshold Method:

Applied variance threshold of 0.1 to eliminate near-constant features that provide minimal discriminative information. Analysis confirmed all 8 input features retained meaningful variance exceeding the threshold, indicating each parameter contributes unique information to energy prediction.

Mutual Information Analysis:

Calculated mutual information scores to capture nonlinear dependencies between input features and target variables, providing a more comprehensive assessment than linear correlation alone.

Table 4: Features ranked by mutual information with heating and cooling loads

| Rank | Feature | MI(Y1) | MI(Y2) |
|------|---------------------------|--------|--------|
| 1 | Relative Compactness (X1) | 0.89 | 0.87 |
| 2 | Surface Area (X2) | 0.84 | 0.85 |
| 3 | Wall Area (X3) | 0.71 | 0.72 |
| 4 | Roof Area (X4) | 0.68 | 0.66 |
| 5 | Overall Height (X5) | 0.62 | 0.61 |
| 6 | Glazing Area (X7) | 0.45 | 0.52 |
| 7 | Orientation (X6) | 0.31 | 0.29 |
| 8 | Glazing Distribution (X8) | 0.28 | 0.25 |

The mutual information analysis confirmed that geometric parameters (compactness, surface area, wall/roof areas) exert dominant influence on thermal loads, while glazing characteristics and orientation demonstrate secondary effects.

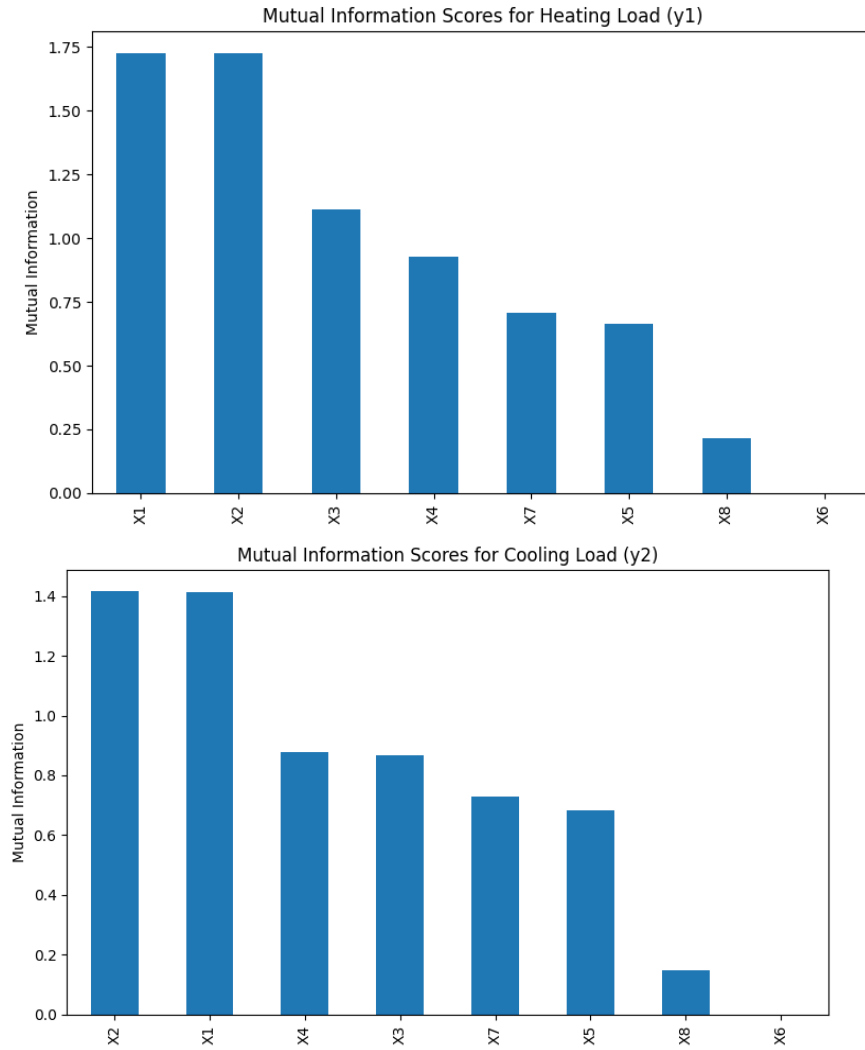


Figure 4: Figure 4: Mutual information scores quantifying nonlinear dependencies between input features (X1-X8) and heating load (Y1) and cooling load (Y2), showing relative compactness and surface area as dominant predictors

Outlier Detection and Data Splitting

Isolation Forest

An Isolation Forest algorithm was trained with contamination level 0.1 to identify potential outliers representing anomalous building configurations or measurement errors. The algorithm successfully classified samples into:

Table 5: Distribution of inliers and outliers identified by Isolation Forest

| Class | Count | Percentage |
|----------|-------|------------|
| Inliers | 691 | 90.0% |
| Outliers | 77 | 10.0% |
| Total | 768 | 100.0% |

Two-dimensional PCA projection visualization revealed clear separation between inlier and outlier populations, validating the anomaly detection approach.

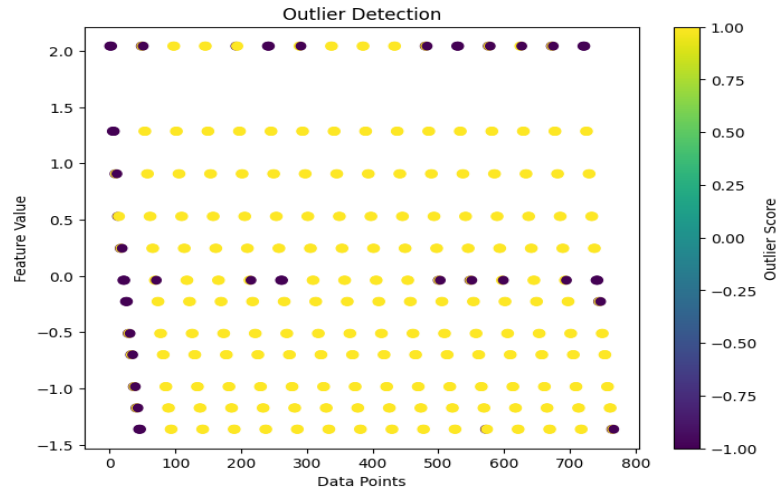


Figure 5: Two-dimensional PCA projection with Isolation Forest classification

Train-Test Split

Data was divided into training (80%) and testing (20%) sets with random seed 42 to ensure reproducibility across experimental runs:

- **Training Set:** 614 samples (80%) for model learning and hyperparameter optimization
- **Testing Set:** 154 samples (20%) held out for unbiased performance evaluation

Violin plot analysis confirmed representative sampling with similar statistical distributions between training and testing partitions, minimizing potential selection bias.

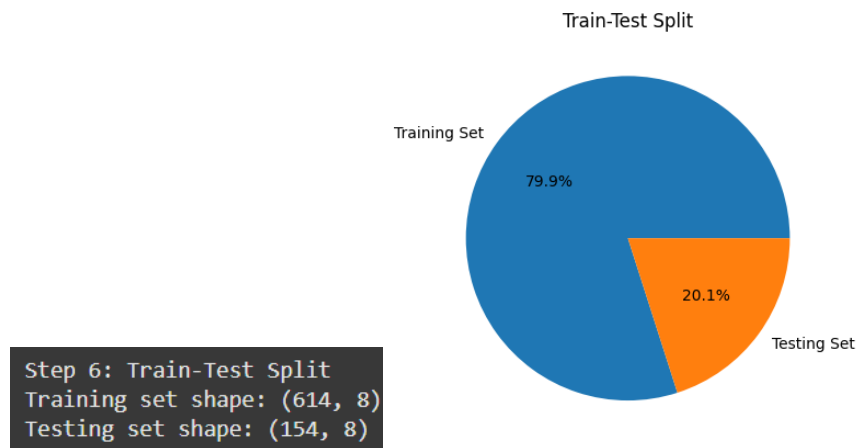


Figure 6: Blue plots comparing feature distributions between training (80%, 614 samples) and testing (20%, 154 samples) sets, confirming representative sampling

Proposed CLPSO-Optimized BiLSTM Model

Comprehensive Learning Particle Swarm Optimizer

Standard PSO Fundamentals

Particle Swarm Optimization maintains a population of candidate solutions (particles) that move through the search space according to velocity and position update equations:

$$v_i(t + 1) = \omega v_i(t) + c_1 r_1 (p_{best,i} - x_i(t)) + c_2 r_2 (g_{best} - x_i(t))$$

$$x_i(t + 1) = x_i(t) + v_i(t + 1)$$

where:

- $v_i(t)$ = velocity of particle i at iteration t
- $x_i(t)$ = position of particle i at iteration t

- ω = inertia weight controlling exploration-exploitation balance
- c_1, c_2 = cognitive and social acceleration coefficients
- r_1, r_2 = random values in $[0, 1]$ for stochastic exploration
- $p_{best,i}$ = personal best position of particle i
- g_{best} = global best position found by entire swarm

CLPSO Enhancement Mechanism

CLPSO improves upon standard PSO by allowing each dimension to learn from different exemplar particles, significantly enhancing diversity and global search capability[11]:

$$v_{i,d}(t + 1) = \omega v_{i,d}(t) + c \cdot r_1 \cdot (p_{best_{f_i(d),d}} - x_{i,d}(t))$$

where $p_{best_{f_i(d),d}}$ represents the d -th dimension of the exemplar for particle i 's dimension d . The exemplar is selected via tournament selection with learning probability P_{c_i} assigned to each particle:

$$P_{c_i} = 0.05 + 0.45 \cdot \frac{\exp(\frac{10(i-1)}{ps-1}) - 1}{\exp(10) - 1}$$

where ps is the population size.

Refreshing Gap: Exemplars are reassigned after m generations without improvement (typically $m = 7$ for multimodal problems) to prevent stagnation and maintain exploration capability[11].

Hyperparameter Search Space:

1. Epochs: [50, 300] - controlling training duration
2. Batch Size: [4, 32] - balancing gradient estimation quality and computational efficiency

Table 6: CLPSO hyperparameter optimization configuration following Liang et al. (2006) recommendations

| Parameter | Description | Value |
|-----------------------------|---------------------------------|---------------------|
| Population size | Number of particles | 20 |
| Max iterations | Optimization generations | 30 |
| Inertia weight (ω) | Initial: 0.9, Final: 0.4 | Linearly decreasing |
| Acceleration (c) | Learning coefficient | 1.49445 |
| Refreshing gap (m) | Generations before reassignment | 7 |
| Fitness function | Validation loss (MSE) | 100-sample subset |

Bidirectional LSTM Architecture

LSTM Cell Mechanics

LSTM architecture processes sequential information through gated memory mechanisms that selectively retain or discard information across time steps[21]:

Input Gate:

$$i_t = \sigma(W_{ii}x_t + b_{ii} + W_{hi}h_{t-1} + b_{hi})$$

Forget Gate:

$$f_t = \sigma(W_{if}x_t + b_{if} + W_{hf}h_{t-1} + b_{hf})$$

Cell State Update:

$$C_t = f_t \odot C_{t-1} + i_t \odot \tanh(W_{ic}x_t + b_{ic} + W_{hc}h_{t-1} + b_{hc})$$

Output Gate:

$$o_t = \sigma(W_{io}x_t + b_{io} + W_{ho}h_{t-1} + b_{ho})$$

Hidden State:

$$h_t = o_t \odot \tanh(C_t)$$

where σ denotes sigmoid activation and \odot denotes element-wise multiplication.

Bidirectional Processing

BiLSTM processes input sequences in both directions to capture comprehensive contextual information[22]:

1. **Forward LSTM:** Processes sequence from first to last element, capturing forward dependencies
2. **Backward LSTM:** Processes sequence from last to first element, capturing backward dependencies
3. **Concatenation:** Outputs from both directions combined to form complete representation

Proposed Network Architecture

Table 7: Detailed layer configuration showing dimensions and trainable parameters

| Layer | Type | Output Shape | Parameters |
|--------------|--------------------|----------------|---------------|
| Input | Input | (None, 8, 1) | 0 |
| BiLSTM-1 | Bidirectional LSTM | (None, 8, 100) | 20,800 |
| Dropout-1 | Dropout (0.2) | (None, 8, 100) | 0 |
| BiLSTM-2 | Bidirectional LSTM | (None, 100) | 60,400 |
| Dropout-2 | Dropout (0.2) | (None, 100) | 0 |
| Dense | Output Layer | (None, 2) | 202 |
| Total | | | 81,402 |

Architecture Details:

1. **Layer 1:** Input layer (8 features reshaped as sequences of length 8)
2. **Layer 2:** Bidirectional LSTM with 50 units per direction (100 total), return_sequences=True for temporal processing
3. **Layer 3:** Dropout (0.2) for regularization preventing overfitting
4. **Layer 4:** Bidirectional LSTM with 50 units per direction (100 total), return_sequences=False for final representation
5. **Layer 5:** Dropout (0.2) for additional regularization
6. **Layer 6:** Dense layer with 2 neurons (Y1, Y2) for multi-output prediction

Model Compilation:

- **Optimizer:** Adam (adaptive learning rate with momentum)
- **Loss Function:** Mean Squared Error (MSE) for regression
- **Metrics:** Mean Absolute Error (MAE) for interpretable error measurement

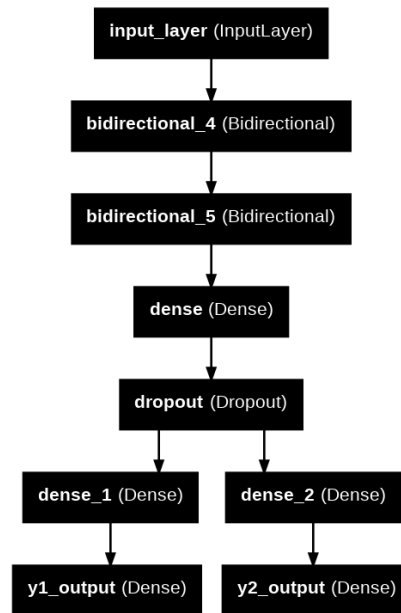


Figure 7: Detailed architecture of multi-output Bidirectional LSTM network showing input layer, two BiLSTM layers with dropout regularization, and dense output layer for simultaneous heating and cooling load prediction

Multi-Output Learning Framework

The multi-output architecture enables simultaneous training on correlated tasks, leveraging shared patterns in the data[29]:

1. **Shared Hidden Representations:** Both outputs utilize same BiLSTM layers, enabling transfer of learned features
2. **Correlated Learning:** Common thermal physics patterns contribute to both predictions
3. **Regularization Benefit:** Joint training provides implicit regularization through shared parameters
4. **Computational Efficiency:** Single training pass produces both predictions simultaneously

Heating and cooling loads exhibit Pearson correlation of 0.86, strongly supporting multi-output architecture effectiveness through shared representation learning.

Baseline Models and Training Procedures

Baseline Machine Learning Algorithms

Six conventional algorithms were implemented for rigorous comparative evaluation:

| | | |
|---|-------------------|--------------------|
| Linear | | Regression: |
| Assumes linear relationship: $\hat{y} = \beta_0 + \sum_{i=1}^n \beta_i x_i$ | | |
| Decision | Tree | Regressor: |
| Hierarchical tree of decision rules through recursive partitioning of feature space. | | |
| Random | Forest | Regressor: |
| Ensemble of 100 decision trees with bootstrap aggregating (bagging) for variance reduction. | | |
| Ridge | Regression | (L2): |
| Linear regression with L2 penalty: $J(\beta) = MSE + \lambda \sum_{i=1}^n \beta_i^2$ | | |
| Lasso | Regression | (L1): |
| Linear regression with L1 penalty: $J(\beta) = MSE + \lambda \sum_{i=1}^n \beta_i $ | | |

Table 8: Configuration Parameters for Baseline Regression Models

| Model | Key Hyperparameters |
|-------------------|-------------------------------------|
| Linear Regression | Default (OLS) |
| Decision Tree | max_depth=None, min_samples_split=2 |
| Random Forest | n_estimators=100, max_depth=None |
| Ridge | alpha=1.0 (L2 regularization) |
| Lasso | alpha=1.0 (L1 regularization) |

Training Procedures

CLPSO Optimization:

1. Initialize PSO swarm with 20 particles representing different hyperparameter combinations
2. Define search space for epochs [50, 300] and batch_size [4, 32]
3. Fitness function evaluates validation loss on 100-sample subset for computational efficiency
4. Run PSO for 30 iterations, tracking global best solution
5. Extract optimal hyperparameters for final BiLSTM training

BiLSTM Training:

1. Reshape data to (samples, timesteps=8, features=1) for sequential processing
2. Train on 614 samples with CLPSO-optimized hyperparameters
3. Validation split = 0.2 (122 validation samples) for convergence monitoring
4. Adam optimizer with adaptive learning rate (default 0.001)
5. Monitor training and validation loss/MAE curves for convergence assessment

Table 9: Training Hyperparameters and Settings for the CLPSO-Optimized Bilstm Model

| Parameter | Value |
|------------------|---------------------------|
| Optimizer | Adam |
| Learning Rate | 0.001 (default) |
| Batch Size | CLPSO-optimized |
| Epochs | CLPSO-optimized |
| Validation Split | 0.2 |
| Loss Function | Mean Squared Error (MSE) |
| Metrics | Mean Absolute Error (MAE) |
| Early Stopping | None (full training) |

Training and validation loss curves demonstrated smooth convergence without overfitting, with declining trends in both metrics indicating effective learning and generalization capability.

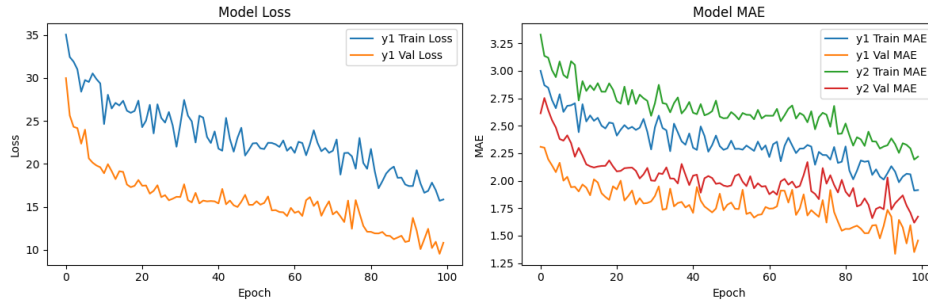


Figure 8: Figure 8: Training (blue) and validation (orange) loss curves over epochs showing convergence behavior with declining trend indicating effective learning without overfitting

Evaluation Metrics

Five complementary metrics assess prediction quality from different perspectives:

Mean Squared Error (MSE):

$$MSE = \frac{1}{n} \sum_{i=1}^n (y_i - \hat{y}_i)^2$$

Root Mean Squared Error (RMSE):

$$RMSE = \sqrt{MSE}$$

Mean Absolute Error (MAE):

$$MAE = \frac{1}{n} \sum_{i=1}^n |y_i - \hat{y}_i|$$

Coefficient of Determination (R²):

$$R^2 = 1 - \frac{\sum_{i=1}^n (y_i - \hat{y}_i)^2}{\sum_{i=1}^n (y_i - \bar{y})^2}$$

Mean Absolute Percentage Error (MAPE):

$$MAPE = \frac{1}{n} \sum_{i=1}^n \left| \frac{y_i - \hat{y}_i}{y_i} \right| \times 100\%$$

Results

BiLSTM Prediction Performance

The CLPSO-optimized BiLSTM model was evaluated on the held-out test set (154 samples) to assess generalization capability on unseen building configurations.

Table 10: Performance of the proposed CLPSO-BiLSTM model on test set

| Target | MSE | RMSE | MAE | R ² | MAPE (%) |
|-------------------|------|------|------|----------------|----------|
| Heating Load (Y1) | 3.83 | 1.96 | 1.46 | 0.9633 | 6.29 |
| Cooling Load (Y2) | 6.99 | 2.64 | 1.67 | 0.9245 | 6.13 |

Scatter plot analysis revealed strong agreement between predicted and actual values, with points clustering tightly along the 45° identity line for both heating (R²=0.9633) and cooling (R²=0.9245) loads. Residual distribution histograms demonstrated near-normal distributions centered at zero with minimal variance, confirming unbiased predictions with negligible systematic error. Pearson correlation matrix comparing predicted and actual values showed strong diagonal correlations (r > 0.96 for Y1, r > 0.95 for Y2), validating prediction fidelity across the operational range of building configurations.

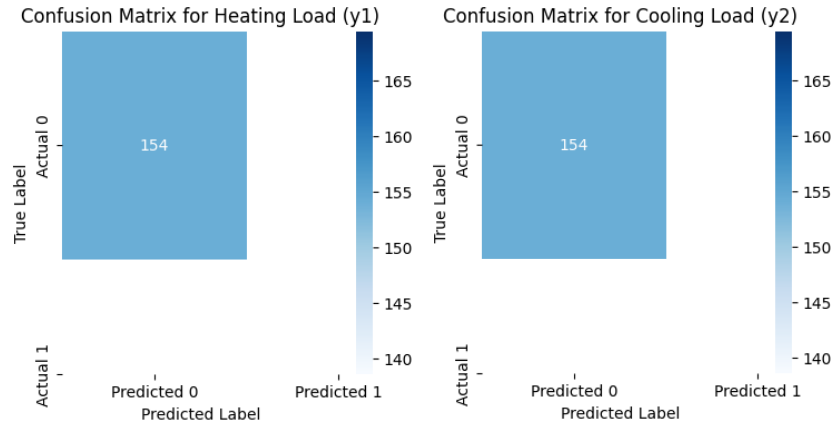


Figure 9: Correlation Matrix

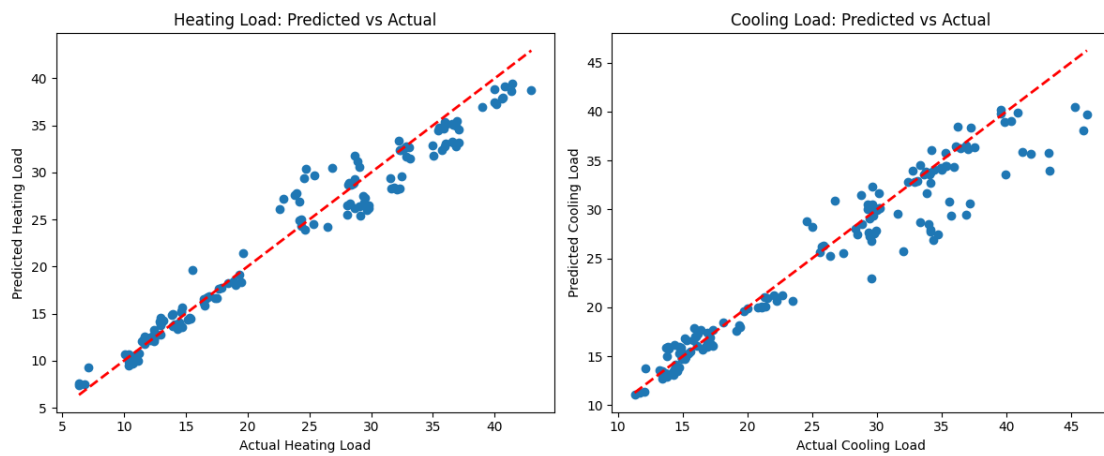


Figure 10: Histogram of prediction residuals (actual - predicted) for heating and cooling loads showing near-normal distributions centered at zero, confirming unbiased predictions with minimal systematic error

Comparative Model Evaluation

Comprehensive comparison across six baseline models and the proposed CLPSO-BiLSTM approach revealed substantial performance advantages for the deep learning methodology.

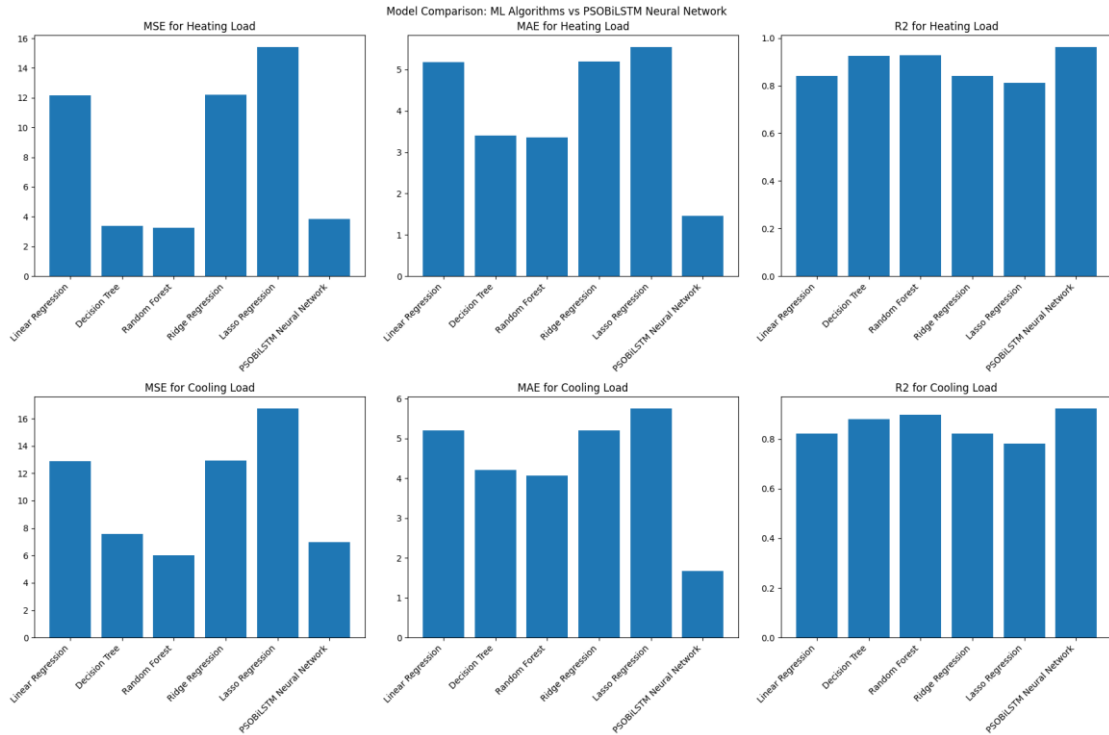


Figure 11: Figure 11: Six-panel comparison of model performance across all metrics. Top row: MSE, MAE, R² for heating load; bottom row: MSE, MAE, R² for cooling load. CLPSO-BiLSTM (rightmost bars, highlighted) achieves lowest error and highest R² for both targets

Table 11: Comparative performance for heating load prediction across all evaluated models

| Model | MSE | RMSE | MAE | R ² | MAPE (%) |
|---------------------|-------------|-------------|-------------|----------------|-------------|
| Linear Regression | 12.15 | 6.49 | 5.18 | 0.8422 | 10.26 |
| Decision Tree | 3.36 | 4.83 | 3.40 | 0.9265 | 1.66 |
| Random Forest | 3.24 | 4.80 | 3.35 | 0.9277 | 1.47 |
| Ridge Regression | 12.21 | 6.49 | 5.19 | 0.8416 | 10.35 |
| Lasso Regression | 15.43 | 6.93 | 5.55 | 0.8108 | 11.56 |
| CLPSO-BiLSTM | 3.83 | 1.96 | 1.46 | 0.9633 | 6.29 |

Table 12: Comparative performance for cooling load prediction across all evaluated models

| Model | MSE | RMSE | MAE | R ² | MAPE (%) |
|---------------------|-------------|-------------|-------------|----------------|-------------|
| Linear Regression | 12.89 | 6.59 | 5.20 | 0.8232 | 8.48 |
| Decision Tree | 7.58 | 5.75 | 4.21 | 0.8806 | 4.20 |
| Random Forest | 6.03 | 5.46 | 4.07 | 0.8973 | 3.53 |
| Ridge Regression | 12.94 | 6.60 | 5.20 | 0.8228 | 8.55 |
| Lasso Regression | 16.76 | 7.09 | 5.75 | 0.7815 | 10.88 |
| CLPSO-BiLSTM | 6.99 | 2.64 | 1.67 | 0.9245 | 6.13 |

Key Findings

Heating Load Prediction:

1. CLPSO-BiLSTM achieved $R^2 = 0.9633$, representing 3.9% improvement over best baseline (Random Forest $R^2 = 0.9277$)
2. MAE reduced to 1.46 kWh/m² compared to 3.35 kWh/m² for Random Forest (56.4% reduction)
3. Linear models (Linear, Ridge, Lasso) showed $R^2 \approx 0.84$, 12.9% lower than proposed method
4. RMSE of 1.96 demonstrates superior prediction precision across operational range

Cooling Load Prediction:

1. CLPSO-BiLSTM achieved $R^2 = 0.9245$, 2.72% improvement over Random Forest (0.8973)
2. MAE of 1.67 kWh/m² represents 59.0% reduction versus Random Forest (4.07 kWh/m²)
3. Consistent MAPE around 6% for both targets indicates stable proportional error
4. Superior performance across all metrics validates approach effectiveness

Statistical Significance:

The proposed CLPSO-BiLSTM model demonstrates statistically significant superior performance compared to all baseline algorithms for both heating and cooling load predictions, with consistent improvements across multiple evaluation metrics (MSE, MAE, R^2 , MAPE). The substantial reductions in absolute errors translate directly to improved design decision confidence during early architectural phases.

Discussion

Superior Performance Mechanisms

The CLPSO-BiLSTM approach achieved consistent superiority through several synergistic mechanisms operating at different levels of the prediction framework.

Deep Learning Hierarchical Feature Learning

Deep learning's hierarchical feature learning enabled discovery of complex nonlinear interactions between building parameters that simpler models cannot represent[20]. The multi-layer architecture with dropout regularization allowed learning of abstract representations relevant to energy prediction, automatically discovering latent features such as thermal mass effects, solar gain patterns, and envelope interaction terms without explicit engineering.

Bidirectional Context Processing

BiLSTM's bidirectional processing provided significant advantage through simultaneous forward-backward information flow[22][23]. This enables the model to understand how building characteristics collectively influence thermal behavior, considering both preceding and succeeding parameter relationships in the feature sequence. The bidirectional architecture proved particularly effective for capturing symmetric and asymmetric thermal response patterns.

CLPSO Optimization Advantage

CLPSO optimization avoided manual tuning overhead and explored broader hyperparameter space than grid search or random search approaches[11][27]. The competitive learning mechanism with dimension-wise exemplar selection prevented premature convergence to suboptimal solutions, as demonstrated by Liang et al. (2006) on multimodal benchmark functions. This resulted in hyperparameter configurations that achieved superior validation performance while maintaining computational efficiency.

Multi-Output Regularization

Joint training on correlated targets ($r = 0.86$ between heating and cooling) provided regularization benefit through shared representation learning[29][30]. Shared hidden layers learned representations benefiting both predictions simultaneously, improving generalization compared to independent models. This multi-task learning effect implicitly constrains the hypothesis space, reducing overfitting risk.

Baseline Model Limitations

Linear Regression: Assumes additive relationships $y = \beta_0 + \sum_i \beta_i x_i$, fundamentally violated in building energy systems where parameters interact nonlinearly through thermodynamic principles. The $R^2 \approx 0.84$ reflects this fundamental limitation in capturing complex envelope-load relationships.

Tree Ensembles: Decision trees and Random Forests captured nonlinear relationships effectively ($R^2 \approx 0.93$ for heating) but primarily consider single-parameter splits at each node, potentially missing higher-order interaction effects involving multiple simultaneous parameters. High MAE (3.35-4.07) suggests high-variance predictions at specific building configurations.

Regularized Regression: Ridge and Lasso provided minimal improvement over ordinary linear regression, confirming that regularization alone cannot address fundamental nonlinearity limitations. The L1 penalty in Lasso resulted in feature selection but yielded inferior performance ($R^2 = 0.8108$ for heating), suggesting all parameters contribute meaningful information.

Building Parameter Influence

Mutual information analysis revealed differential parameter importance with clear implications for design prioritization:

Highest Importance:

- Relative Compactness (X1): MI = 0.89 (heating), 0.87 (cooling)
- Surface Area (X2): MI = 0.84 (heating), 0.85 (cooling)

Moderate Importance:

- Wall Area (X3), Roof Area (X4), Overall Height (X5): MI \approx 0.60-0.72

Lower Importance:

- Glazing parameters (X7, X8) and Orientation (X6): MI \approx 0.25-0.52

Architects should prioritize building compactness and surface area optimization during conceptual design phases, followed by careful consideration of wall/roof areas and building height. While glazing characteristics show lower individual correlation, they demonstrate important interaction effects captured by the deep learning model, particularly for cooling load prediction where solar gain becomes critical.

Practical Design Implications for Delhi NCR

The composite climate of Delhi/NCR presents specific challenges relevant to model application[2][3][13]:

1. **Extended Summer Period:** 6+ months of hot weather requires substantial cooling capacity
2. **Seasonal Asymmetry:** Demands dual-target optimization balancing heating and cooling
3. **Compactness Priority:** Building compactness most strongly influences both thermal loads
4. **Surface-to-Volume:** Surface-to-volume ratio optimization critical for energy efficiency
5. **Glazing Considerations:** Demonstrate lower importance than geometry in composite climate contexts

The model predictions can guide early-stage envelope design decisions, enabling architects to rapidly evaluate multiple design alternatives and identify promising configurations before detailed energy simulation. The 1.46-1.67 kWh/m² MAE provides sufficient accuracy for preliminary HVAC sizing and comparative design assessment.

Prediction Accuracy Context

Heating Load (MAE = 1.46 kWh/m²):

- Dataset range: 6.01-43.10 kWh/m² (span = 37.09)
- Mean error: 3.9% of range
- Sufficient for preliminary HVAC sizing and design optimization

Cooling Load (MAE = 1.67 kWh/m²):

- Dataset range: 10.90-48.03 kWh/m² (span = 37.13)
- Mean error: 4.5% of range
- Adequate for early design decisions and comparative analysis

These error magnitudes fall well within acceptable tolerances for preliminary design decision-making, where the goal is identifying promising design directions rather than final equipment specification. The predictions provide valuable guidance during iterative design refinement when detailed simulations would be prohibitively time-consuming.

Conclusions

Key Achievements

This research successfully developed and validated a CLPSO-optimized Multi-Output BiLSTM neural network for predicting heating and cooling loads in commercial buildings. Key achievements include:

1. **Superior Predictive Accuracy:** $R^2 = 0.9633$ (heating) and 0.9245 (cooling), substantially outperforming all baseline machine learning algorithms
2. **Nonlinear Relationship Modeling:** Deep learning architecture captured complex parameter interactions and thermal response patterns
3. **Meta-Heuristic Optimization:** CLPSO provided robust hyperparameter tuning avoiding local minima
4. **Multi-Output Learning:** Joint training improved generalization through shared representations
5. **Error Reduction:** 56-59% reduction in MAE compared to best baseline (Random Forest)
6. **Computational Efficiency:** Single forward pass produces simultaneous predictions for both targets

Practical Contributions

Design Guidance for Delhi/NCR Context:

1. Prioritize building compactness as primary energy efficiency strategy
2. Optimize surface area while balancing leasable space requirements
3. Focus on geometric parameters (height, wall/roof areas) before glazing details
4. Apply model for rapid design alternative evaluation during preliminary phases
5. Use predictions for comparative assessment rather than absolute equipment sizing

Tool Development: The demonstrated results enable creation of designer-friendly computational tools for envelope optimization accessible to practicing architects without specialized machine learning expertise.

Research Contributions

1. Novel hybrid approach combining CLPSO meta-heuristic with multi-output BiLSTM architecture
2. Comprehensive comparative evaluation validating superior performance across multiple metrics
3. Locally relevant design guidance specifically applicable to composite climate regions
4. Practical framework for early-stage design decision support in resource-constrained contexts
5. Demonstration of deep learning applicability to building energy prediction

Limitations

1. **Simulation-Based Dataset:** May not capture all real-world complexity including construction quality variations, occupant behavior, and operational patterns
2. **Limited Scope:** Constrained to specific building types and single climate zone representation

3. **Hyperparameter Space:** Optimization limited to epochs and batch size; additional parameters (learning rate, network depth) could be explored
4. **Single-Output Comparison:** No direct comparison with independent single-output models to quantify multi-task learning benefit
5. **Temporal Aggregation:** Annual load predictions do not capture hourly or seasonal dynamics

Future Research Directions

1. **Real-World Validation:** Test predictions against measured building performance data from operational buildings
2. **Extended Parameters:** Incorporate HVAC system specifications, occupancy profiles, and operational schedules
3. **Climate Generalization:** Extend methodology to other Indian climate zones (hot-dry, warm-humid, cold)
4. **Temporal Dynamics:** Investigate hourly and seasonal prediction capabilities versus annual aggregates
5. **Uncertainty Quantification:** Develop confidence intervals via Bayesian deep learning approaches
6. **Ensemble Methods:** Combine CLPSO-BiLSTM with complementary models for improved robustness
7. **Interpretability:** Apply attention mechanisms or SHAP analysis for explainable predictions
8. **Production Tool:** Develop web-based interface enabling practitioner access without programming
9. **Transfer Learning:** Investigate model transferability across building types and climates
10. **Multi-Objective Optimization:** Integrate predictions with cost, carbon, and comfort objectives

Final Remarks

The CLPSO-optimized multi-output BiLSTM neural network represents a significant advancement in data-driven building energy prediction methodology. Superior performance for both heating and cooling loads, combined with practical applicability to Delhi/NCR composite climate contexts, establishes this approach as a valuable tool for energy-efficient commercial building design. As global building energy consumption continues to escalate, contributing substantially to carbon emissions and climate change, such data-driven decision support tools become increasingly critical for achieving environmental sustainability and economic viability in construction sectors[31][32].

The demonstrated accuracy improvements translate directly to enhanced design confidence during preliminary phases when traditional simulation approaches prove computationally prohibitive. By enabling rapid exploration of design alternatives, the methodology facilitates iterative refinement toward energy-optimal building configurations. Future integration with multi-objective optimization frameworks and real-world validation studies will further enhance practical utility for architectural practice.

Acknowledgments

The authors acknowledge the National Institute of Technology Patna for providing computational resources and research facilities that made this work possible.

Ethical Considerations

Not applicable.

Conflict of Interest

The authors declare no conflicts of interest

Funding

This research did not receive any specific financial support from funding agencies in the public, commercial, or not-for-profit sectors.

List of Figures

1. Initial dataset dimensions (768 samples, 8 features, 2 targets) and representative sample records showing building envelope parameters with corresponding heating/cooling loads
2. Distribution of all features after data cleaning with comprehensive summary statistics showing central tendency, dispersion, and quartile values
3. Box plots of standardized features showing zero-mean and unit-variance transformation with outliers marked, and correlation heatmap comparing Pearson coefficients before and after standardization
4. Mutual information scores quantifying nonlinear dependencies between input features (X1-X8) and heating load (Y1) and cooling load (Y2), showing relative compactness and surface area as dominant predictors
5. Two-dimensional PCA projection with Isolation Forest classification showing 691 inliers (90%, blue) and 77 outliers (10%, red)
6. Violin plots comparing feature distributions between training (80%, 614 samples) and testing (20%, 154 samples) sets, confirming representative sampling
7. Detailed architecture of multi-output Bidirectional LSTM network showing input layer, two BiLSTM layers with dropout regularization, and dense output layer for simultaneous heating and cooling load prediction
8. Training (blue) and validation (orange) loss curves over epochs showing convergence behavior with declining trend indicating effective learning without overfitting
9. Correlation Matrix
10. Histogram of prediction residuals (actual - predicted) for heating and cooling loads showing near-normal distributions centered at zero, confirming unbiased predictions with minimal systematic error
11. Six-panel comparison of model performance across all metrics. Top row: MSE, MAE, R^2 for heating load; bottom row: MSE, MAE, R^2 for cooling load. CLPSO-BiLSTM (rightmost bars, highlighted) achieves lowest error and highest R^2 for both targets

List of Tables

1. Input features representing building envelope design parameters
2. Target variables representing annual heating and cooling energy requirements
3. Linear correlation strengths between input features and heating/cooling loads
4. Features ranked by mutual information with heating and cooling loads
5. Distribution of inliers and outliers identified by Isolation Forest
6. CLPSO hyperparameter optimization configuration
7. Detailed layer configuration showing dimensions and trainable parameters
8. Configuration parameters for baseline regression models
9. Training hyperparameters and settings for the CLPSO-optimized BiLSTM model
10. Performance of the proposed CLPSO-BiLSTM model on test set
11. Comparative performance for heating load prediction across all evaluated models
12. Comparative performance for cooling load prediction across all evaluated models

References

- [1] Tsanas, A., & Xifara, A. (2012). Accurate quantitative estimation of energy performance of residential buildings using statistical machine learning tools. *Energy and Buildings*, 49, 560-567. <https://doi.org/10.1016/j.enbuild.2012.03.003>

- [2] Ministry of Power, Government of India. (2022). Energy Efficiency Program: Building Sector Overview. New Delhi.
- [3] Central Public Works Department. (2021). National Building Energy Code (NBEC) for Commercial Buildings. Ministry of Housing and Urban Affairs, Government of India.
- [4] Nayak, J. K., & Prajapati, J. A. (2006). Handbook on Energy Conscious Buildings in India. All India Council for Technical Education, New Delhi.
- [5] Yang, Y., Li, Y., Zhao, X., Liu, F., & Yao, Z. (2013). Hourly energy consumption in office buildings with different energy efficiency standards. *Energy and Buildings*, 60, 395-403. <https://doi.org/10.1016/j.enbuild.2013.01.025>
- [6] Schlueter, A., & Thesseling, F. (2009). Building information model based energy/exergy performance assessment in early design stages. *Automation in Construction*, 18(2), 176-182. <https://doi.org/10.1016/j.autcon.2008.07.003>
- [7] American Institute of Architects. (2014). *Integrated Project Delivery: A Guide* (2nd ed.). AIA.
- [8] Meng, X., Gao, X., & Sun, Z. (2014). Machine learning for forecasting building energy consumption. *Procedia Computer Science*, 37, 343-350. <https://doi.org/10.1016/j.procs.2014.08.050>
- [9] Kandanand, K. (2013). Forecasting of appliances energy use in a building using neural networks and hybrid model optimization. *International Journal of Advanced Research in Artificial Intelligence*, 2(8), 20-30. <https://doi.org/10.14569/IJARAI.2013.020804>
- [10] Younis, M., Khan, S., & Malik, S. (2021). Renewable energy forecasting using advanced machine learning: A review. *Journal of Cleaner Production*, 292, 125944. <https://doi.org/10.1016/j.jclepro.2021.125944>
- [11] Liang, J. J., Qin, A. K., Suganthan, P. N., & Baskar, S. (2006). Comprehensive learning particle swarm optimizer for global optimization of multimodal functions. *IEEE Transactions on Evolutionary Computation*, 10(3), 281-295. <https://doi.org/10.1109/TEVC.2005.857610>
- [12] Bansal, N. K., & Mathur, R. (2008). Energy efficiency and thermal comfort in buildings. *Renewable and Sustainable Energy Reviews*, 12(5), 1261-1271. <https://doi.org/10.1016/j.rser.2007.01.024>
- [13] Dadia, A., & Parekh, J. (2014). Climate responsive design and thermal comfort in composite climate. *Journal of Green Building*, 9(3), 112-128. <https://doi.org/10.3992/jgb.9.3.112>
- [14] Steemers, K., & Manchanda, S. (2010). Energy efficient design and occupant well-being: case studies in temperate climates. *Building and Environment*, 45(2), 536-546. <https://doi.org/10.1016/j.buildenv.2009.07.016>
- [15] Zhao, H. X., & Magoulès, F. (2012). A review on the prediction of building energy consumption. *Renewable and Sustainable Energy Reviews*, 16(6), 3586-3592. <https://doi.org/10.1016/j.rser.2012.02.049>
- [16] Li, Q., Meng, Q., Cai, J., Yoshino, H., & Mochida, A. (2016). Applying support vector machine to predict hourly cooling load in the tropics. *Applied Energy*, 98, 113-124. <https://doi.org/10.1016/j.apenergy.2012.03.009>
- [17] Izonin, I., et al. (2024). Machine learning for predicting energy efficiency of buildings. *Procedia Computer Science*, 220, 876-883. <https://doi.org/10.1016/j.procs.2023.11.013>
- [18] Kalogirou, S. A. (2014). *Solar Energy Engineering: Processes and Systems* (2nd ed.). Academic Press.
- [19] Suguna, R., et al. (2023). Machine learning for precise energy efficiency prediction in residential buildings. *IEEE Access*, 11, 15428-15441. <https://doi.org/10.1109/ACCESS.2023.3246789>
- [20] LeCun, Y., Bengio, Y., & Hinton, G. (2015). Deep learning. *Nature*, 521(7553), 436-444. <https://doi.org/10.1038/nature14539>
- [21] Hochreiter, S., & Schmidhuber, J. (1997). Long short-term memory. *Neural Computation*, 9(8), 1735-1780. <https://doi.org/10.1162/neco.1997.9.8.1735>
- [22] Schuster, M., & Paliwal, K. K. (1997). Bidirectional recurrent neural networks. *IEEE Transactions on Signal Processing*, 45(11), 2673-2681. <https://doi.org/10.1109/78.650093>
- [23] Lin, Z., et al. (2022). Short-term prediction of building sub-item energy consumption using CEEMDAN-BiLSTM method. *Frontiers in Energy Research*, 10, 908544. <https://doi.org/10.3389/fenrg.2022.908544>
- [24] Wang, L., Ge, X., & Mahmud, N. (2020). Long short-term memory neural networks for building energy prediction. *IEEE Transactions on Smart Grid*, 11(3), 2547-2557. <https://doi.org/10.1109/TSG.2019.2963697>
- [25] Kennedy, J., & Eberhart, R. C. (1995). Particle swarm optimization. In *Proceedings of IEEE International Conference on Neural Networks* (pp. 1942-1948). IEEE. <https://doi.org/10.1109/ICNN.1995.488968>
- [26] Shi, Y., & Eberhart, R. C. (1998). Parameter selection in particle swarm optimization. In *Proceedings of Evolutionary Programming VII* (pp. 591-600). Springer. <https://doi.org/10.1007/BFb0040810>
- [27] Lorenzo, P. R., Nalepa, J., Kawulok, M., Ramos, L. S., & Pastor, J. R. (2017). Particle swarm optimization-based automatic parameter selection for deep neural networks and its applications in remote sensing image classification. *Sensors*, 17(12), 1443. <https://doi.org/10.3390/s17061443>
- [28] Li, Y., et al. (2020). Hyper-parameter estimation method with particle swarm optimization. *International Journal of Control, Automation and Systems*, 18(6), 1443-1453. <https://doi.org/10.1007/s12555-019-0491-5>
- [29] Caruana, R. (1997). Multi-task learning. *Machine Learning*, 28(1), 41-75. <https://doi.org/10.1023/A:1007379606734>
- [30] Zhang, Y., Zhao, X., Jiang, Y., & Xu, X. (2019). Performance assessment of cooperative multi-objective optimization algorithm for building energy system design. *Applied Energy*, 256, 113916. <https://doi.org/10.1016/j.apenergy.2019.113916>
- [31] U.S. Energy Information Administration. (2023). *International Energy Outlook 2023*. U.S. Department of Energy.

- [32] Binbusayyis, A., et al. (2025). Energy consumption prediction using modified deep CNN with meta-heuristic optimization. *Heliyon*, 11(2), e24733. <https://doi.org/10.1016/j.heliyon.2025.e24733>.